CONF-8704178--1

DE87 011147

Theoretical Aspects of High-Energy Heavy-Ion Reactions

Cheuk-Yin Wong

Oak Ridge National Laboratory
Oak Ridge, Tennessee 37830
U.S.A.

Lectures presented at the 10th INS-Kikuchi Spring School on Quarks and Nuclei, Shimoda, Japan, April 1987

We present here an elementary introduction to the subject of nucleus-nucleus collisions at high energies. It begins with a discussion on the relevant kinematic variables to establish the language for these collisions. It examines the question of particle production and the characteristics of the loss of baryon energy in an inelastic nucleon-nucleon collision. The geometrical aspect of a nucleus-nucleus collision is then described in terms of the Glauber multiple-collision model. As the theory of relativistic heavy-ion collision has not yet reached a stage whereby the dynamics can be examined from a fundamental theory, various phenomenological models have been proposed. The assumptions used in various models are described. Future use of relativistic heavy-ion collisions to study the quark-gluon plasma is briefly discussed.

I. INTRODUCTION

Recently, there is much interest in relativistic heavy-ion collisions which stems from the possibility of creating matter with very high energy densities.[1] The energy densities may be high enough to exceed the critical energy density for a phase transition from the ordinary confined hadronic matter to the unconfined quark-gluon plasma. Experimental searches and identification of the quark-gluon plasma may provide new insight into the question of quark confinement. Furthermore, the creation of the domain of high energy density, albeit within a small region of space and time, may allow one to study matter under unusual conditions such as those which exist in the history of the early universe.

We expect the occurrence of high energy density regions in heavy-ion reactions for the following reasons. It is known that in a high-energy nucleon-nucleon collision, the nucleons lose much of their energy and a large number of particles are produced. A nucleus-nucleus collision consists of many nucleon-nucleon collisions. Qualitatively speaking, the effect of the nucleon-nucleon collisions in a nucleus-nucleus reaction is roughly additive in nature. Furthermore, because of Lorentz contraction, these nucleon-nucleon collisions occur at about the same time in about the same spatial region (in the center-of-mass system). There is, therefore, a cooperative slowing-down of the baryons and a nearly simultaneous production of overlapping domains of high energy densities to lead to regions of very high energy densities.

We expect the occurrence of high energy density regions in two different situations: in the "stopping" region at about a few GeV per nucleon in the C.M. system, and in the "central rapidity" region at the higher energy of about 100 GeV per nucleon in the center-of-mass system. In the first situation, we envisage the collective slowing-down of the baryons in the center-of-mass frame so that the the nuclear matter is nearly stopped in that

frame. The type of quark-gluon plasma which may be formed in this region is a baryon-rich quark-gluon plasma. At higher energies, the baryons cannot be completely stopped. They are slowed down but still proceed forward in the C.M. frame after inelastic collisions. When the baryons are well separated, the energy which is trapped between the colliding nucleons may become liberated in the region between receding baryons, the "central rapidity" region. The additive effect of many such colliding nucleons may produce a quark-gluon plasma with small baryon content. As the net baryon content of the early universe is very small[2], this type of quark-gluon plasma is of special astrophysical interest.

A quantitative understanding of the detailed dynamics of nucleus-nucleus collisions is useful for an assessment of the possibility of quark-gluon plasma formation. The knowledge of the dynamics will also help one separate out the signals which are expected in the hadronic phase and the signals which are peculiar in the quark-gluon plasma phase. We need to know how a baryon may be slowed down in its passage through a nucleus and how particles are produced in a nuclear environment. How the heavy-ion collisions proceed is the subject of current investigations and will be the main focus of the present lecture here.

High-energy heavy-ion physics is an emerging field, both experimentally and theoretically. The development is still in a state of flux. Many models have been proposed and many more may yet come as the problem is not completely solved. It is appropriate to review the status of present research and to prepare here a set of tools so that newcomers can make use of these tools to make contributions in this area. For this purpose, simple problems are posted in the lecture notes.

II. KINEMATIC VARIABLES

In relativistic heavy-ion collisions, as well as in nucleon-nucleon collisions, it is convenient to use kinematic variables with suitable properties under Lorentz transformations. The light-cone variable x, the rapidity variable y, and the pseudo-rapidity variable η are kinematic variables which are commonly used. It is worthwhile to discuss these variables in some detail to establish the proper language to describe relativistic collisions.

In many processes, a particle c can be identified as originating from or related to another parent particle b. For example, in the reaction $b + a \to c + X$, the detected particle c can sometimes be considered as fragmenting from the incident beam particle b. The light-cone variable x is introduced to specify the relationship between the four-momentum of the daughter particle c and the four-momentum of the parent beam particle b. In these reactions, quantities along the direction of the incident beam, which we call the longitudinal axis, have properties quite different from those along the transverse directions perpendicular to the beam axis. We shall designate the z-axis as the longitudinal axis. In terms of the energy c_0 and the longitudinal momentum c_z , the light-cone variable x is defined as

$$x = \frac{c_0 + c_z}{b_0 + b_z} \tag{2.1}$$

where we use the same symbol to represent a particle and its four-momentum. That is, $c = (c_0 , \vec{c})$ and $b = (b_0 , \vec{b})$. Under a change of the Lorentz frame, the numerator in Eq. (2.1) transforms in the same way as the denominator. Therefore, the light-cone variable x is independent of the Lorentz frame. This variable is sometimes called the forward light-cone variable and is denoted by x_+ when we want to distinguish it from the backward light-cone

variable x_- appropriate for target fragmentation.

At very high energies when the energy and the longitudinal momentum are approximately the same, the light-cone variable x is just the longitudinal momentum fraction of the daughter particle c relative to the parent particle b. For this reason, the variable x is sometimes called the longitudinal momentum fraction or simply the momentum fraction of c relative to b.

The daughter particle c may be a particle detected as a free particle in an apparatus. In this case, the particle is not subject to interactions and its four-momentum obeys the on-the-mass-shell relation:

$$c^2 = c_0^2 - \vec{c}^2 = m_c^2 \tag{2.2}$$

where m_c is the rest mass of c. The four-momentum c now has only three degrees of freedom, and it can be represented by $(x,\vec{c}_T)$ where $\vec{c}_T$ is the transverse momentum of particle c. There is a simple transformation which gives $(c_0,\vec{c})$ in terms of $(x,\vec{c}_T)$ (Problem 2.1).

In some problems, particle c is not a free and detected particle and is still subject to interactions in the fragmenting system. The four-momentum of c will not obey the on-the-mass-shell relation (Eq. 2.2). Its four degrees of freedom can be specified by the Lorentz invariant quantities $(x, \vec{c}_T, c^2)$ where $c^2 = c_0^2 - \vec{c}^2$ or by $(x_+, x_-, \vec{c}_T)$.

Problem 2.1

Show that when particle c is on the mass shell, c_0 and c_z are related to x by

$$c_0 = \frac{1}{2}\left[x(b_0+b_z) + \frac{m_T^2}{x\,(b_0+b_z)} \right]$$

and

$$c_z = \frac{1}{2}\left[x(b_0+b_z) - \frac{m_T^2}{x\,(b_0+b_z)} \right]$$

where $m_T^2 = m_c^2 + \vec{c}_T^2$.

Problem 2.2

The Feynman scaling variable x_F for a detected particle c is defined as

$$x_F = \frac{c_z^*}{c_{max}^*}$$

where the asterisk stands for the center-of-mass system. By going to the center-of-mass system, show that in the case of very high energies, the light-cone variable x coincides with the Feynman scaling variable. Note, however, that the light-cone variable differs from the Feynman scaling variable when c_z^* is small or negative.

L_____

The light-cone variable x introduced in Eq. (2.1) is useful when we want to describe the particle c in terms of the fragmentation of the beam particle b. Fragmentation of this type is called a projectile fragmentation reaction. There are situations where we wish to consider a particle c as originating from the target particle a. Fragmentation of this type is called a target fragmentation reaction. In that case, it is convenient to define the backward light-cone variable x_- appropriate for the target fragmentation region as

$$x_- = \frac{c_0 - c_z}{a_0 - a_z} \qquad (2.3)$$

The light-cone variable x_- is also independent of the Lorentz frame, and it obeys relations similar to those given above for the light-cone variable x. It gives the longitudinal momentum fraction of particle c relative to the parent particle a. As the variables x_+ and x_- are independent of the frame of reference, it is often convenient to work with light-cone momentum coordinates $p_+ = c_0 + c_z$ and $p_- = c_0 - c_z$ instead of c_0 and c_z. The ratio of the light-cone momentum coordinate of the daughter particle to that of the parent particle gives then the momentum fraction carried by

the particle.

Another useful variable in common use to describe the kinematic condition of a detected particle is the rapidity variable y. It is defined in terms of its momentum by

$$y = \frac{1}{2} \ln \frac{c_0 + c_z}{c_0 - c_z} \qquad (2.4)$$

The rapidity variable depends on the frame of reference, but the dependence is very simple (Problem 2.3). The rapidity of one frame of reference is related to the rapidity in another frame of reference by an additive constant.

Problem 2.3

Show that under a Lorentz transformation from a laboratory frame to a frame moving with velocity ß, (for simplicity, we shall use units in which $c = h = 1$.), the rapidity of the particle in the new frame y' is related to y by

$$y' = y - y_0$$

where

$$y_0 = \frac{1}{2} \ln \frac{1 + ß}{1 - ß} .$$

Prove that y_0 is the rapidity the particle will have if it travels with the velocity ß in the laboratory frame.

Problem 2.4

In the collision of a (beam) nucleon with momentum b_z on a target nucleon a at rest, show that the initial rapidities of the particles are

$$y_a = 0 ,$$

and

$$y_b = \sinh^{-1}(b_z / m_N).$$

where m_N is the nucleon rest mass. Show that a nucleon traveling with the velocity of the center-of-mass frame has a rapidity given

by

$$y_{cm} = (y_a + y_b) /2 .$$

Thus, in the nucleon-nucleon center-of-mass frame

$$y_a^* = -(y_b - y_a)/2 , \quad \text{and} \quad y_b^* = (y_b - y_a)/2 .$$

The simple property of the rapidity variable under Lorentz transformation makes it a suitable choice to describe the dynamics of relativistic particles. To go from one frame of reference to another frame of reference, it is only necessary to find the rapidity y_0 corresponding to the moving frame in question and change the rapidity variables by this additive constant. This is similar to the situation in non-relativistic kinematics where the longitudinal velocity in one frame is related to the logitudinal velocity in another moving frame by an additive constant. This similarity is not a surprising result because non-relativistically, y is equal to the longitudinal velocity v_z.

For a given incident energy, the projectile particles and the target particles have definite rapidities (Problem *2.4*). The region in between the projectile rapidity and the target rapidity is called the central rapidity region. The rapidity of the produced particles lies mostly in this region.

If the particle c is a free particle, then it is on the mass shell. Its four-momentum has only three degrees of freedom and can be represented by $(y, \vec{c}_T)$. There is a simple transformation which gives $(c_0, \vec{c})$ in terms of $(y, \vec{c}_T)$ (Problem 2.5).

Problem 2.5

Show that if c is on the mass shell, then c_0 and c_z are related to y by

$$c_0 = m_T \cosh y ,$$

and

$$c_z = m_T \sinh y .$$

From the definitions of x and y, it is easy to show that

$$x = \frac{m_T}{m_b} e^{y-y_b}, \tag{2.5}$$

and conversely,

$$y = y_b + ln\ x + ln\ (m_b / m_T) \ . \tag{2.6}$$

These relations also indicate that a complete description of the full dynamical range requires both the x and the y variable. Specifically, for reactions leading to particles with momentum close to that of the incident beam, the light-cone variable x is a more appropriate quantity to use. A projectile fragmentation reaction is characterized by detecting particles with the light-cone variable close to unity. In this region, the rapidity variable changes only slightly and is relatively insensitive to a large change of longitudinal momentum. On the other hand, for those particles detected with a momentum fraction small compared with the momentum of the incident beam, a small region of the light-cone variable x is transformed into a large region in the rapidity variable y. To examine these particles in these regions, the rapidity variable y is a more appropriate kinematic variable. We shall use these two variables interchangeably as the situation warrants.

Experimentally, a particle c is often characterized by the pseudo-rapidity variable η which is defined as

$$\eta = - ln\ [\ tan\ (\theta / 2)\ ] \tag{2.7}$$

where θ is the laboratory angle of the detected particle. In terms of the momentum, the pseudo-rapidity variable can be written as

$$\eta = \frac{1}{2}\ ln \frac{|\vec{c}| + c_z}{|\vec{c}| - c_z} \tag{2.8}$$

It is easy to see that the pseudo-rapidity variable coincides with the rapidity variable when the momentum is large.

Problem 2.6

Show that the variable y and η are related by

$$y = \frac{1}{2} \ln \frac{\sqrt{p_T^2 \cosh^2\eta + m_T^2} + p_T \sinh \eta}{\sqrt{p_T^2 \cosh^2\eta + m_T^2} - p_T \sinh \eta},$$

and conversely,

$$\eta = \frac{1}{2} \ln \frac{\cosh y \sqrt{1 - m^2 / m_T^2 \cosh^2 y} + \sinh y}{\cosh y \sqrt{1 - m^2 / m_T^2 \cosh^2 y} - \sinh y}.$$

Show that if particles have a distribution dN/dy in terms of the rapidity variable y, then the distribution in the pseudo-rapidity variable η is

$$\frac{dN}{d\eta} = \sqrt{1 - m^2 / m_T^2 \cosh^2 y} \frac{dN}{dy}.$$

Show that in the region of y much greater than 0, $dN/d\eta$ and dN/dy are approximately the same, but in the region y close to 0, there is a small depression of the distribution $dN/d\eta$ due to the transformation. (In collider experiments at high energies when dN/dy has a plateau shape, this transformation gives a small 'dip' in $dN/d\eta$ around $\eta \approx 0$.[3,4])

III. NUCLEON-NUCLEON COLLISIONS

The search for exotic behavior of quark-gluon plasma requires a comparison with what is expected from normal behavior without the contributions from the quark-gluon plasma sources. It is therfore useful to work out what is expected from "normal" collisions. Whether or not the energy density is high enough for a phase transition also requires an understanding of the dynamics of nucleus-nucleus collisions which remains a subject under investigation. Attempts have been made to relate the nucleus-nucleus results to those from nucleon-nucleon collisions. In relativistic nucleus-nucleus collisions, there are peculiarities of the collisions which arise from the relativistic nature of the process so that a nucleon-nucleon collision in a nucleus need not be the same as that in free space. Nevertheless, information from nucleon-nucleon collisions provides valuable data and concepts for nucleus-nucleus collisions. For this reason, it is useful to discuss the physics of nucleon-nucleon collisions in some detail.

3.1 Particle Production in Nucleon-Nucleon Collisions

The nucleon-nucleon inelastic cross-section is approximately 32 mb which is relatively energy independent[5]. About 6% of this can be attributed to diffractive dissociation for which the leading particle loses very little energy. Elastic or diffractive dissociation collisions lead to a small loss of the energy of the nucleons. Thus, for our discussion of particle production and stopping of baryons, two nucleons undergoing elastic or diffractive dissociation collisions can be considered as suffering essentially no collision at all. On this basis, we shall consider only non-diffractive inelastic collisions unless specified otherwise. For simplicity, by a nucleon-nucleon collision, we shall mean a non-diffractive inelastic

nucleon-nucleon collision with a cross-section σ_{in} of about 30 mb.

Inelastic collisions at high energies are characterized by the production of a large number of particles, most of which are pions[3,5]. The mechanism leading to particle production is qualitatively understood[6-8] as arising from the Schwinger mechanism in which the two colliding particles form a strong constant-force field between them, much like the case of a linear string. Particle-antiparticle pairs are produced by one particle tunneling from the negative energy sea to the positive energy continuum, leaving a hole in the negative energy sea in one region and a particle in the positive continuum in another region. The physics of such a phenomenon can be illustrated with a simple example of Klein-Gordon particles in a constant-force field of finite dimensions (Problem 3.1). (The more exact, but more complicated case of Dirac particles in a constant-force field with a finite dimension has been solved[9]. However, for simplicity, it will not be discussed here).

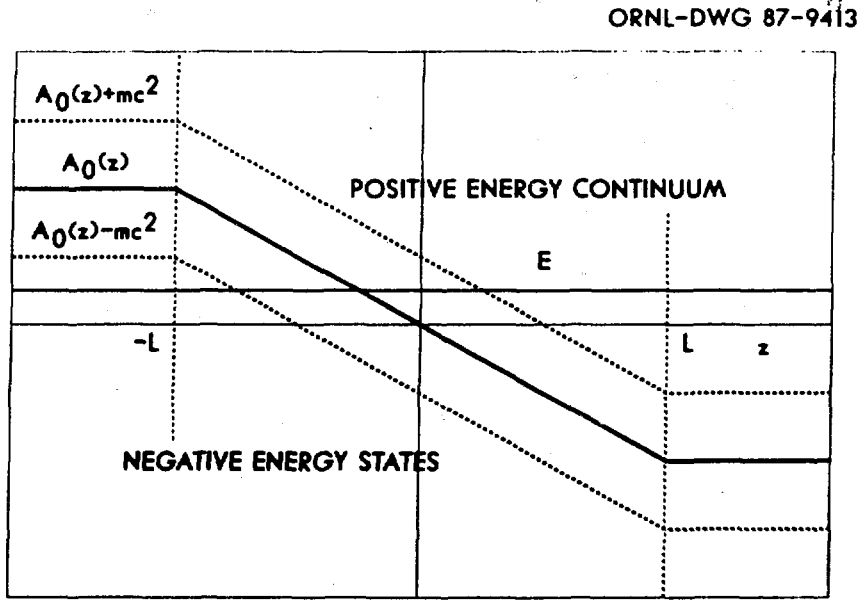

Fig. 1. The potential $A_0(z)$.

Problem 3.1

Consider a particle with a mass m in a static linear vector potential $A = (\vec{0}, A_0)$ of the form (Figure 1):

$$A_0 = \begin{cases} kL & \text{for } z \le -L \\ -kz & \text{for } -L \le z \le L \\ -kL & \text{for } L \le z \end{cases} .$$

The Klein-Gordon equation for the particle is

$$\left[(p - A)^2 - m^2 \right] \psi = 0 .$$

Show that by making the transformation

$$\xi = \sqrt{2} \; [\; E + k(z-L) \;] / \sqrt{k}$$

where E is the energy of the particle, the equivalent Schrödinger equation is formally the same as that in the tunneling of an inverted parabolic barrier. The tunneling is permitted for states in the interval

$$-kL + mc^2 \le E \le kL - mc^2 .$$

Show by the WKB method that the penetrability for a negative energy state at $E=0$ to tunnel to the positive energy continuum is

$$P = exp \; (-2\pi a)$$

where

$$a = (m^2 + \vec{p}_T^{\,2})/2k .$$

With this result, show that in the vicinity of $z=0$, the production rate for a pair per unit volume per unit time is

$$w = \frac{k^2}{8\pi^2} \, e^{-\pi m^2/k}$$

which is identical to the Schwinger[6] result.

L-------

The results in Problem (3.1) indicates that the transverse momentum serves to provide an effective transverse mass to the particle and this effective mass must likewise tunnel through the barrier. It must work against the field and is therefore limited by the field strength k to result in a transverse momentum

distribution of the form $exp\ (-\pi\ \vec{p}_T^{\,2}/k)$. It also shows that there is no particle production if the length of the string $2L$ is less than $2m/k$. If one takes the quark mass to be[10] about 350 MeV, and the string tension k to be 1 GeV/fm, then the minimum length required for particle production is 0.7 fm for a particle with $p_T=0$ but increases to 1 fm for a quark with a transverse momentum of 0.35 GeV.

The above static problem (Problem 3.1) contains exact solutions[11] which involve parabolic cylinder functions[12]. Numerical solutions show that the penetrability has spatial oscillations for finite systems. As expected, the smaller the system, the greater is the amplitude of oscillation.

The problem we discuss is one with the geometry of a parallel plate. One may well ask on what basis can it be applied to nucleon-nucleon collisions which are better described by a flux tube of radius R. For a transverse momentum greater than about h/R and in the interior of the tube, the wave equation can be approximated to be that for the parallel plate. However, for small transverse momenta, it is necessary to take into account the boundary condition in the transverse directions and the solution of the parallel plate will not be appropriate there. As yet, how particles are produced in a flux tube geometry has not been studied.

Although a numerical solution of the problem posted in Prob. 3.1 has been obtained, and the spatial variation of particle prodution probability has been calculated, the solutions cannot yet be applied quantitatively to nucleon-nucleon collisions at high energies. For the latter collisions, the end points of the linear force field move with high velocities which will affect particle production. We are now studying how this time dependence may affect particle production.

Much insight in particle production mechanism is provided by examining a 1+1 dimensional QED problem with massless fermions in which a charge fermion (a quark, say) and its anti-particle pulls

apart with the speed of light.[7] It is known that because of the gauge property of the field, the 1+1 dimensional QED with massless fermions is equivalent to a scalar field with a massive scalar particle. The scalar particle can be thought of as a fermion-antifermion pair[13]. The motion of the end-point fermions creates a time-dependent dipole field between them which acts as an external field to excite these fermion-antifermion pairs into the continuum. Applied to the problem of particle production in nucleon-nucleon or in $e^+ e^-$ collisions, one obtains the following space-time description of the dynamics when a quark q and anti-quark $\bar{q}$ pull away from each other[7,8]. When the separation between the quark q and the anti-quark $\bar{q}$ is greater than a certain length (of the order of 0.5-1.0 fm, say), a pair of quark-antiquark $q_1\bar{q}_1$ will be produced. The produced $\bar{q}_1$ will travel toward q while the produced q_1 will travel toward $\bar{q}$, with $\bar{q}q_1$ and $\bar{q}_1 q$ forming two separated strings. In the separated strings, as the end points of the strings are still pulling apart, further production of $q\bar{q}$ pairs will break the string into more pieces until each string is separated into a yo-yo state[14] (Problem 3.2) which can be considered as a relatively long-lived

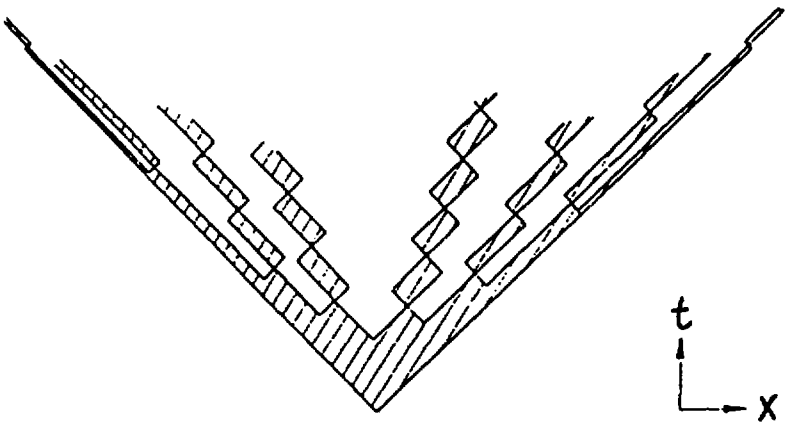

Figure 2. Inside-outside cascade picture of particle production.

resonance. This process starts from the creation of a pair in the inside region between the two separating particles and follows with the breaking of the strings in the outside region. It is called the inside-outside cascade picture of particle production.[15,7] (Figure 2)

Problem 3.2

Consider a massless quark pair q_1-$\bar{q}_2$ with the following Hamiltonian,

$$H = |\vec{p}_1| + |\vec{p}_2| + k\,|x_1 - x_2| \ .$$

Initially, both quarks are at the origin and have momenta $p_1(0)$ and $p_2(0) < 0$. (Figure 3)

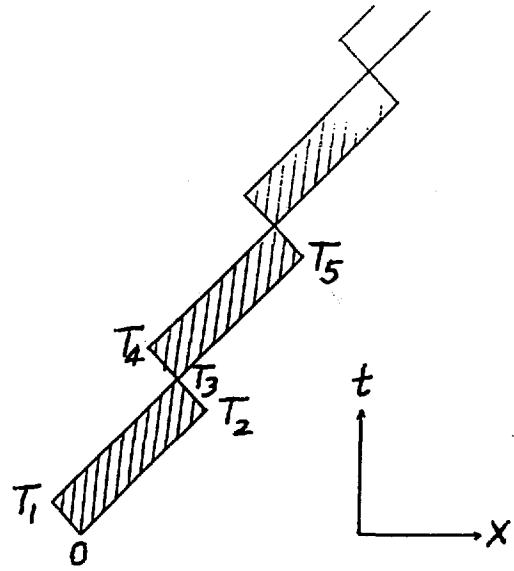

Figure 3. Space-time dynamics of a yo-yo state.

Use the Hamilton's canonical equation to show that the velocities and momenta of these two particles are

$$\dot{x}_1(t) = \begin{cases} 1 & \text{for} \quad t \le T_2 \\ -1 & \text{for} \quad T_2 \le t \le T_4 \end{cases}$$

$$\dot{x}_2(t) = \begin{cases} -1 & \text{for} \quad t \le T_1 \\ 1 & \text{for} \quad T_1 \le t \le T_5 \end{cases}$$

$$p_1(t) = \begin{cases} -kt + p_1(0) & \text{for} \quad t \le T_2 \\ -k(t-T_2) & \text{for} \quad T_2 \le t \le T_3 \\ -k(t+T_2-2T_3) & \text{for} \quad T_3 \le t \le T_4 \end{cases}$$

and

$$p_2(t) = \begin{cases} +kt + p_2(0) & \text{for} \quad t \le T_1 \\ +k(t-T_1) & \text{for} \quad T_1 \le t \le T_3 \\ -k(t+T_1-2T_3) & \text{for} \quad T_3 \le t \le T_5 \end{cases}$$

where

$$T_1 = -p_2(0)/k \ , \quad T_2 = p_1(0)/k \ , \quad T_3 = T_2+T_1$$

$$T_4 = T_2 + 2T_1, \quad \text{and} \quad T_5 = T_1 + 2T_2 \ .$$

Problem 3.3

Consider a massless q_1-$\bar{q}_2$ pair with q_1 moving initially in the forward direction with momentum $p_1(0)$ and $\bar{q}_2$ moving in the backward direction with momentum $p_2(0)$. The Hamiltonian is given by H in Problem 3.2. At time t_0, a pair $\bar{q}_3$-q_4 is created with zero momentum. (Figure 4)

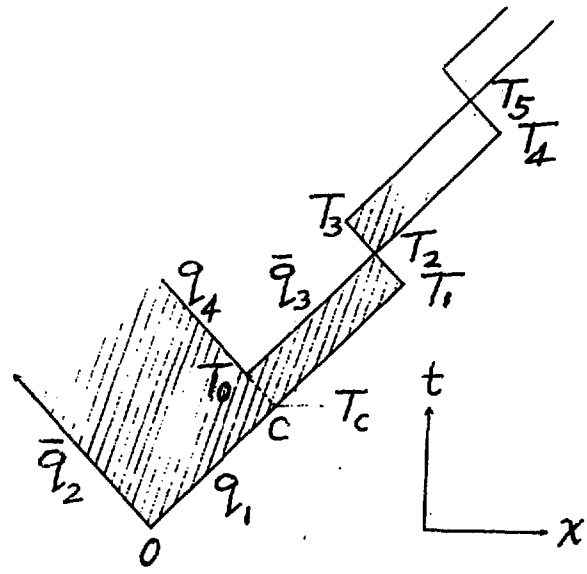

Fig. 4 Space-time dynamics after the creation of the $\bar{q}_3$-q_3 pair

The Hamiltonian becomes

$$H = |p_1| + |p_2| + |p_3| + |p_4| + k\,|x_1 - x_3| + k\,|x_2 - x_4| \quad .$$

Show that the time dependence of the velocities and momenta of q_1 and $\bar{q}_3$ are:

$$\dot{x}_1 = \begin{cases} 1 & \text{for} \quad t \le T_1 \\ -1 & \text{for} \quad T_1 \le t \le T_3 \\ 1 & \text{for} \quad T_3 \le t \le T_5 \end{cases}$$

$$\dot{x}_3 = \begin{cases} 1 & \text{for} \quad T_0 \le t \le T_4 \\ -1 & \text{for} \quad T_4 \le t \le T_5 \end{cases}$$

$$p_1(t) = \begin{cases} -kt + p_1(0) & \text{for} \quad t \le T_1 \\ -k(t-T_1) & \text{for} \quad T_1 \le t \le T_2 \\ -k(2T_2 - t - T_1) & \text{for} \quad T_2 \le t \le T_3 \\ k(t-T_3) & \text{for} \quad T_3 \le t \le T_5 \end{cases}$$

and

$$p_3(t) = \begin{cases} k(t-T_0) & \text{for} \quad T_0 \le t \le T_2 \\ k(2T_2 - t - T_0) & \text{for} \quad T_2 \le t \le T_4 \\ -k(t-T_4) & \text{for} \quad T_4 \le t \le T_5 \end{cases} \quad .$$

Note that the dynamics of these two quarks q_1 and $\bar{q}_3$ are the same if they originate from the point C at T_c (Figure 4) with momenta $p_3(T_c) = -k(T_0 - T_c)$ and $p_1(T_c) = k(T_1 - T_c)$.

In the dynamical case with the end points moving away from each other, the probability distribution of the momentum fraction carried by the produced pair has not been worked out quantum mechanically from a theoretical viewpoint. Many phenomenological models have been put forth to specify the distribution $f(x)$ of the location of the light-cone variable x for one of the two particles in the intermediate $q\bar{q}$ pairs. For example, there is the Feynman-Field parametrization[16],

$$f(x) = 1 - a + 3a\,(1-x)^2$$

with a value of $a \cong 0.77$. The SLAC formula[17] gives a distribution,

$$f(x) = \frac{1}{x}\left\{1 - \frac{1}{x} - \frac{\epsilon}{1-x}\right\}^2$$

where ϵ is a reference scale. On the other hand, the Lund model[7] assumes a distribution of the form

$$f(x) = \frac{1}{x}\, x^{a_\alpha}\left[\frac{1-x}{x}\right]^{a_\beta} exp\left\{-\frac{b\, m^2}{x} T\right\}$$

where a_α , a_β , and b are free parameters. This form of distribution was based on the requirement that it gives a rapidity distribution of produced particles which has a plateau shape at high energies and that the distribution is the same whether the string is broken from the left or from the right. A good fit to experimental data can be obtained with $a_\alpha = a_\beta = 1$ and $b = 0.7$ GeV^{-2}.

The most extensive numerical investigation of the above space-time development of a q-$\bar{q}$ pair has been carried out by the Lund group.[8] In their calculations, one starts with either end of the q-$\bar{q}$ system and the distribution $f(x)$ gives the location of the vertex which divides the system into two parts (as in Problem 3.3). One part is considered an excited hadron resonance (a yo-yo state) while the other part will undergo further fragmentation with the same probability function $f(x)$ to divide the string into more parts. The division is stopped when the available energy of the string is lower than a certain limit. Phenomenologically, the Lund model has achieved a considerable degree of success.

As is well known, for a given total energy loss, the multiplicity distribution in pp collisions is wider than the multiplicity distribution in e^+e^- collisions[18]. The particle production mechanism which works in e^+e^- collisions is different from the mechanism in pp collisions. The above scheme which is directly applicable to e^+e^- collisions, needs to be modified to make it applicable to hadron-hadron collisions. A new version of the Lund model has been proposed[19,20] in which the hadrons under an inelastic collision are assumed to exchange momentum and become

two independent and excited clusters. The probability distribution for the exchanged momentum is taken to be a particular form. After the exchange of momentum, the two clusters each decay into hadrons in accordance with the space-time dynamics of the $q\text{-}\bar{q}$ evolution as in the earlier version of the Lund model. A generalization of this "independent excitation" scheme has been used for heavy-ion collisions[19,20].

Experimental data[4] of nucleon-nucleon collisions reveal that about 90% of the produced particles are pions; the rest consists of kaons, baryons, anti-baryons and other particles. Their average transverse momentum is about 350 Mev/c which is increased slightly at very high energies[4]. The total multiplicity of particles increases with the C.M. energy approximately in a logarithmic way. The rapidity distribution is in the form of a bell-shaped curve for $\sqrt{s} \simeq 10$ GeV, but at the ISR energies with $\sqrt{s}$ up to 63 GeV, the rapidity distribution dN/dy of the produced charged particles assumes the shape of a plateau having a value of about 2 in the central rapidity region.

For many practical applications, it is desirable to parametrize the particle production data in terms of simple functions. There is now a good collection of experimental data to permit a simple parametrization. In the $p+p \rightarrow \pi^{\pm} + X$ reaction, the momentum distribution of the produced pions follows a simple $(1-x)^a$ relation in the projectile fragmentation region[4,5], with $a \approx 3 - 4$. There is a similar distribution for the pions produced in the target fragmentation region. It is convenient to parametrize the rapidity distribution of the produced charged particles in the following form:

$$dN/dy = A \left[(1 - x_+)(1 - x_-) \right]^a \qquad (3.1)$$

where x_+ is the light-cone variable for projectile fragmentation

$$x_+ = m_{\pi T} \exp (y - y_b) / m_N \quad ,$$

x_- is th light-cone variable for target fragmentation,

$$x_- = m_{\pi T} \exp (y_T - y) / m_N ,$$

and y_b and y_T are the beam and target rapidity variables respectively. The quantity $m_{\pi T}$ is the pion transverse mass and is set equal to $\sqrt{m_\pi^2 + B_T^2}$, where B_T is the average transverse momentum $<|\vec{p}_T|>$ of the produced particles. In this form, the distribution exhibits a $(1-x)^a$ type behavior at the fragmentation regions, a bell-shaped distribution at low energies and a plateau-shaped distribution as energy increases. We find that the following set of parameters[21] gives a satisfactory description of the experimental rapidity distribution of non-leading charged particles:

$$A = 0.75 + 0.38 \ln \sqrt{s} ,$$

$$a = 3.5 + 0.7 \ln \sqrt{s} , \qquad (3.2)$$

and

$$B_T = 0.27 + 0.037 \ln \sqrt{s} ,$$

where B_T is in units of GeV/c and $\sqrt{s}$ in units of GeV. The results obtained by using this set of parameters are shown as solid curves in Figures 5 and 6. There is a good agreement with the $dN/d\eta$ values at the central rapidity region as a function of the center of mass energy $\sqrt{s}$ (Figure 5). There is also a good agreement for the rapidity distribution $dN/d\eta$ at $\sqrt{s}$=540 GeV obtained with the CERN SPS collider[4] (Figure 6). On the other hand, the rapidity distribtuions obtained with this set of parameters are slightly narrower than the rapidity distributions from the CERN ISR experiments[3]. At the ISR energies ($\sqrt{s}$ from 24 to 63 GeV), there is a substantial contribution of the leading baryons to the two wings of $dN/d\eta$. The observed distributions are broader than what is given by the parametrization of Eqs.(3.1,3.2) which includes only non-leading particles. At the much higher energy of the SPS collider, the leading baryons have rapidities much separated from those of the produced particles so that Eqs.(3.1,3.2) can be directly compared with experimental data which presumably do not

include the leading particles.

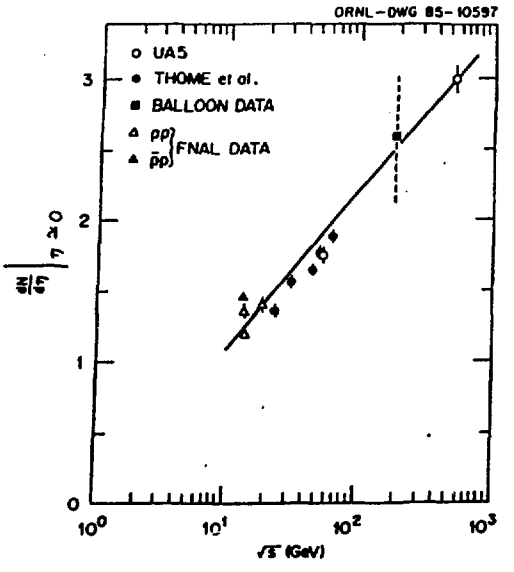

Fig. 5. $dN/d\eta$ data at $\eta \simeq 0$ as a function of $\sqrt{s}$

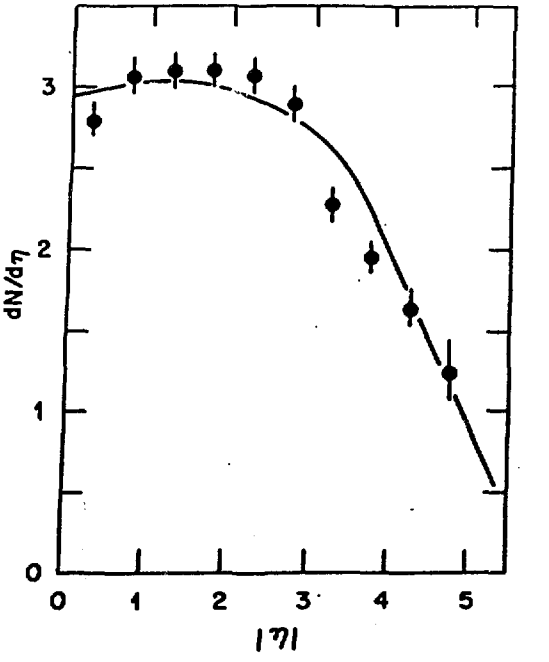

Fig. 6. $dN/d\eta$ as a function of η for $\sqrt{s}$=540 GeV

From the distribution of dN/dy, one can integrate over the rapidity variable to obtain the total multiplicity of non-leading charged particles. Experimental measurements of the total charged multiplicity include also the leading particle and occasionally the target proton. To obtain the total charged multiplicity, we therefore add a constant of 1.5 to the integral of Eq.(3.2) to take into account the contributions from the leading particles. The result is shown as the solid curve in Figure 7. It agrees with experimental total average multiplicity data $\langle n \rangle$.

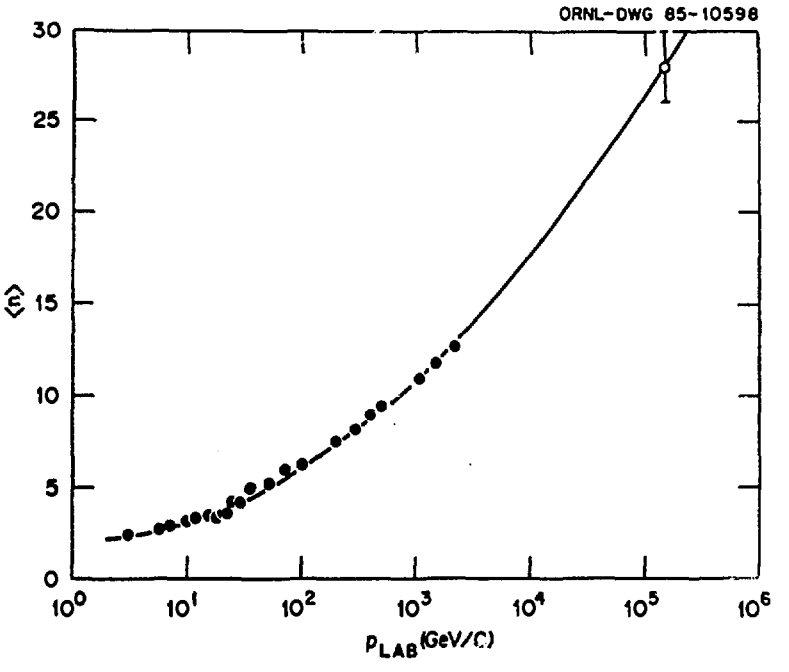

Fig. 7. Total charged multiplicity versus $\sqrt{s}$.

3.2 BARYON ENERGY LOSS IN AN INELASTIC COLLISION

In a nucleon-nucleon or a baryon-baryon inelastic collision, there should be at least two baryons among the product hadrons because of the law of baryon conservation. These baryons are likely to be among the leading particles with one baryon in the projectile fragmentation region and another one in the target fragmentation region. If one considers the detected baryons as related to the corresponding incident baryons, one can view an inelastic collision as a reaction in which an energetic baryon suffers a degradation of its energy after a collision. The degree of inelasticity can be measured by the light-cone variable x defined as the ratio of the light-cone momentum of the detected baryon to that of the incident (parent) baryon [Eq. (2.1)]. For $x > 0$, the light-cone variable x and the Feynman scaling variable x_F nearly coincide. As the phenomenon of Feynman scaling[22] corresponds to the situation when the cross section plotted as a function of the Feynman scaling variable is independent of the

incident energy, the present case of $d\sigma/dx$ being nearly independent of the incident energy for $x \blacktriangleright 0$ can be called the occurrence of Feynman scaling. We show in Figure 8 the experimental inelastic cross-section data[5] for the

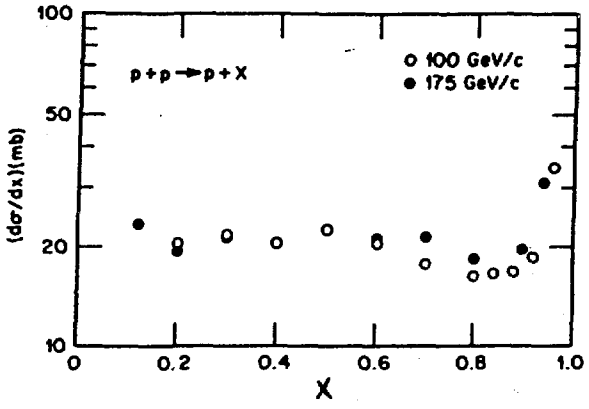

Fig. 8. Experimental cross-section $d\sigma/dx$ for p+p→p+X.

reaction p + p → p + X as a function of x. The distribution $d\sigma/dx$ for $x \blacktriangleright 0$ is nearly independent of the incident energy for an incident momentum of 100 GeV/c and 175 GeV/c (Figure 8). Thus, there is a Feynman scaling for the inelastic cross section when p_{lab} exceeds about 100 GeV/c. A systematic examination of the nucleon-nucleon data shows that Feynman scaling commences at a slightly lower energy of many tens of GeV in the laboratory system[23].

To study the degrees of energy loss in an inelastic collision, we examine the shape of the distribution $d\sigma/dx$ as a function of the light-cone variable x. Except for the diffractive dissociation region in the vicinity of $x \approx 1$, the distribution (i.e. the differential cross section) is nearly flat. If one extrapolates to small regions of x and does not include diffractive dissociation in our consideration (see Section 3.1), an approximate representation of the (differential) cross section

is

$$d\sigma/dx \approx \sigma_{in}\ \theta(\,1-x\,)\ \theta(x-x_L)\ /\ (1-x_L)\quad , \qquad (3.3)$$

where x_L is the lower limit of x as required by energy and momentum consideration. It has a value which is much smaller than unity[24]. [Strictly speaking, the upper limit x_U of x is not unity, but the difference of x_U from unity is small. Furthermore, unlike the lower limit which is very important in setting correctly the lower limit of the rapidity variable, a small variation in the upper limit is of little consequence. We shall take the upper limit as unity.] The distribution (3.3) shows that after an inelastic nucleon-nucleon collision, there is an equal probability of finding a product baryon in the whole range of the light-cone variable. The average value of x is

$$\langle x \rangle = 1/2 \qquad (3.4)$$

Therefore, on the average, the product baryon carries about half of the initial light-cone momentum. This implies that about half of the initial light-cone momentum of the baryon is lost. If the incident baryon carries hundreds of GeV, then the energy-momentum loss can be very substantial in magnitude.

In nucleus-nucleus collisions, the nucleons of one nucleus suffer many collisions with nucleons of the other nucleus. In a multiple-collision process, the loss of the incident energy and momentum can be quite large and may lead to the "stopping" of the baryons in the C.M. system. We shall return to this topic later on.

The production of particles and the loss of baryon energy are intimately related because the total energy of the system must be conserved. There is, in fact, an experimental correlation between the baryon energy loss and the multiplicity of particles produced[25]. The greater the energy loss of the baryons, the greater will be the number of particles produced.

IV. GLAUBER MODEL OF COMPOSITE-PARTICLE COLLISIONS

The Glauber model[26] of multiple-collision processes provides a quantitative consideration of the geometrical sizes of the composite particles when they collide. It is based on the concept of a mean-free path with the assumption of a basic "parton-parton" cross-section. In the naive quark model of a hadron, the partons are just the valence quarks. In a nucleus, the partons are the nucleons. When a parton of one particle passes through the other particle, it may become excited and may, in principle, have a different cross section. We can understand much of the geometrical concepts of the collision process if we take the basic parton-parton cross section to be the same throughout the passage of the parton in the other particle.

We consider the collision of composite particles B and A. We begin by defining $t(b)d\vec{b}$ as the probability for having a parton-parton collision within the transverse area element $d\vec{b}$ when one parton is situated at an impact parameter b relative to another parton. The function $t(b)$ is called the basic parton-parton thickness function. Clearly, the total probability of a collision integrated over all impact parameters is unity and $t(b)$ is normalized according to

$$\int t(b)\ d\vec{b} = 1 \ . \qquad (4.1)$$

We denote the parton-parton basic cross-section (for an inelastic process, with the production of other particles) to be σ_{in} . Thus, when one parton is situated at an impact parameter b relative to the other parton, the probability of having a parton-parton collision is $t(b)\sigma_{in}$.

We define next the probability of finding a parton in the volume element $d\vec{b}_B dz_B$ in particle B at the position $(\vec{b}_B, z_B)$ as $\rho_B(\vec{b}_B, z_B)\ d\vec{b}_B dz_B$ which is normalized according to

$$\int \rho_B(\vec{b}_B, z_B)\ d\vec{b}_B\ dz_B = 1 \ . \qquad (4.2)$$

Note that ρ is equal to the usual number density function divided by the number of partons in the particle. The probability function of finding a parton in the particle A at the position $(\vec{b}_A, z_A)$ can be similarly defined as $\rho_A(\vec{b}_A, z_A)$ and normalized as

$$\int \rho_A(\vec{b}_A, z_A)\, d\vec{b}_A\, dz_A = 1$$

We can now write down the probability for the occurrence of a parton-parton collision when the particles B and A are situated at an impact parameter b relative to each other. We call this probability $T(b)\sigma_{in}$:

$$T(b)\sigma_{in} = \int \rho_A(\vec{b}_A, z_A)\, d\vec{b}_A dz_A\, \rho_B(\vec{b}_B, z_B)\, d\vec{b}_B dz_B\, t(\vec{b} - \vec{b}_A - \vec{b}_B)\, \sigma_{in} ,$$

which defines the thickness function $T(b)$ for the composite particles A and B:

$$T(b) = \int \rho_A(\vec{b}_A, z_A)\, d\vec{b}_A dz_A\, \rho_B(\vec{b}_B, z_B)\, d\vec{b}_B dz_B\, t(\vec{b} - \vec{b}_A - \vec{b}_B) \quad . \qquad (4.3)$$

From Eqs (4.1) and (4.2), the thickness function is normalized according to

$$\int T(b)\, d\vec{b} = 1 \ . \qquad (4.4)$$

The probability for the occurrence of n inelastic parton-parton collisions at an impact parameter b is given by

$$P(n, \vec{b}\,) = \binom{AB}{n} [T(b)\sigma_{in}]^n\, [1 - T(b)\sigma_{in}]^{AB-n} \ . \qquad (4.5)$$

The total probability for the occurrence of an inelastic event in the collision of A and B at an impact parameter $\vec{b}$ is the sum of Eq.(4.5) for n=1 to n=AB :

$$\frac{d\sigma_{in}^{AB}}{d\vec{b}} = \sum_{n=1}^{AB} P(n, \vec{b}) = 1 - [1 - T(b)\sigma_{in}]^{AB} \qquad (4.6)$$

Therefore, the total inelastic cross section σ_{in}^{AB} for the collision of A and B is

$$\sigma_{in}^{AB} = \int d\vec{b} \left\{ 1 - \left[1 - T(b)\sigma_{in} \right]^{AB} \right\} \qquad (4.7)$$

With the probability of having n parton-parton collisions as given by Eq. (4.5), we can find the average number of parton-parton collisions at an impact parameter b as

$$n(b) = \sum_{n=1}^{AB} n\, P(\vec{n},b) = AB\, T(b)\sigma_{in} \qquad (4.8)$$

The average number of parton-parton collision, under the additional condition of the occurrence of an inelastic collision, is

$$n'(b) = AB\, T(b)\sigma_{in} \Big/ \left\{ 1 - [\, 1 - T(b)\sigma_{in}]^{AB} \right\} . \qquad (4.9)$$

When we further average $n'(b)$ over the impact parameter b with the weighting factor of the inelastic differential cross section, we get the average number of parton-parton collisions in an inelastic nucleus-nucleus collision:

$$\langle n \rangle = \frac{\int d\vec{b}\; n'(\vec{b}) \;\{\, 1 - [1 - T(b)\sigma_{in}]^{AB}\}}{\int d\vec{b} \quad \{\, 1 - [1 - T(b)\sigma_{in}]^{AB}\}} . \qquad (4.10)$$

From Eqs. (4.7,4.10), we obtain the mean number of parton-parton collisions in an inelastic collision of the composite particles A and B as

$$\langle n \rangle = AB\, \sigma_{in} / \sigma_{in}^{AB} . \qquad (4.11)$$

The basic thickness function $t(b)$ can be well approximated by a Gaussian function with a standard deviation β_p. If the composite particles are small, their density function ρ can also be taken to be a Gaussian funtion of the spatial coordinates. Consequently, the thickness function of Eq.(4.3) can be conveniently written as

$$T(b) = exp\ (\ -b^2/2\beta^2)\ /2\pi\beta^2 \qquad (4.12)$$

where

$$\beta^2 = \beta_A^2 + \beta_B^2 + \beta_p^2\ .$$

In terms of the standard root-mean-squared-radius parameter r_{rms} for particles A and B, the standard deviation β_A (or, similarly, β_B) is given by

$$\beta_A = r_{rms}\ A^{1/3}/\sqrt{3}\ .$$

The Gaussian form of the thickness function is actually a more general shape than one may at first expect. It turns out that for the collision of two composite particles with a relatively flat spatial density in the shape of a Fermi distribution (as in the case of a heavy nucleus), numerical calculations show that the thickness function can be well approximated by a Gaussian function, except that the effective parameter r_{rms} is slightly larger.[27]

With a Gaussian thickness function, the total inelastic cross section can be obtained as an analytic function. (Problem 4.1)

Problem 4.1

Show that the total inelastic cross section for a Gaussian thickness function is

$$\sigma_{in}^{AB} = 2\pi\beta^2 \sum_{i=1}^{AB} \left[\ 1 - (\ 1 - f\ )^{\,i}\ \right] / i$$

which can also be written as

$$\sigma_{in}^{AB} = -\ 2\pi\beta^2 \sum_{i=1}^{AB} \sum_{j=1}^{i} \left[\begin{matrix} i \\ j \end{matrix} \right] (-f)^j / i$$

where f is a dimensionless quantity given by

$$f = \sigma_{in} / 2\pi\beta^2\ .$$

Prove that if f is small, then

$$\sigma_{in}^{AB} \cong AB\ \sigma_{in} \quad .$$

Problem 4.2

Consider a hadron-nucleus collision with a target mass $A \gg 1$ or a nucleus-nucleus collision with $A \gg B$. The thickness function obtained with a sharp-cutoff density distribution has the form

$$T(b) = (3/2\pi R^3)\ (R^2 - b^2)^{1/2}\ \theta(R-b)$$

where R is the sum of the radii of the two colliding particles. Show that the inelastic cross section is

$$\sigma_{in}^{AB} = \pi R^2 \left\{ 1 + \frac{2}{F^2} \left[\frac{1 - (1-F)^{A+2}}{A+2} - \frac{1 - (1-F)^{A+1}}{A+1} \right] \right\}$$

where F is a dimensionless ratio

$$F = 3\ \sigma_{in} / 2\pi R^2 \quad .$$

The formalism developed above is appropriate for the total number of collisions and the total inelastic cross section. In some problems, it is also necessary to know the history of the collision process, as for example, in the dynamics involving the slowing-down of the baryons. It is convenient to adopt a row-on-row picture of one row of n nucleons from nucleus B colliding with another row of m nucleons in the other nucleus A. We construct the normalized thickness function $T_B(b_B)$ for the nucleus B as

$$T_B(b_B) = T_B(\vec{b}_B) = \int \rho_B(\vec{b}_B, z_B)\ dz_B \quad . \qquad (4.13)$$

The thickness function $T_A(b_A)$ for the other nucleus A can be similarly constructed. The basic unit of area is the nucleon-nucleon inelastic cross section σ_{in}. The probability of finding a nucleon in a tube of cross section σ_{in} at the transverse coordinate $\vec{b}_B$ is $T_B(b_B)\sigma_{in}$. The probability of finding n nucleons in a tube of cross section σ_{in} at the transverse coordinate $\vec{b}_B$ in

nucleus B is given by

$$\binom{B}{n}[T_B(b_B)\sigma_{in}]^n \quad [\,1 - T_B(b_B)\sigma_{in}]^{B-n} \tag{4.14}$$

which has an average value of

$$\langle n(b_B)\rangle = BT_B(b_B)\sigma_{in} \ . \tag{4.15}$$

Similarly, the probability of finding m nucleons in a tube of cross section σ_{in} at the transverse coordinate $\vec{b}_A$ in nucleus A is given by

$$\binom{A}{m}[T_A(b_A)\sigma_{in}]^m \quad [\,1 - T_A(b_A)\sigma_{in}]^{A-m} \tag{4.16}$$

which has an average value of

$$\langle m(b_A)\rangle = AT_A(b_A)\sigma_{in} \ . \tag{4.17}$$

The probability of having a nucleon-nucleon collision in the area element $d\vec{b}_A$ is $t(\vec{b}-\vec{b}_A+\vec{b}_B)d\vec{b}_A$ where $\vec{b}$ is the impact paramater of B relative to A. Putting all the factors together, we find the probability of having n nucleons of B in a tube of cross section σ_{in} colliding with m nucleons of A in a similar tube is

$$P(n,m,\vec{b}_B,\vec{b}) = \int t(\vec{b}-\vec{b}_A+\vec{b}_B)d\vec{b}_A \binom{B}{n}[T_B(b_B)\sigma_{in}]^n \quad [\,1 - T_B(b_B)\sigma_{in}]^{B-n}$$

$$\times \binom{A}{m}[T_A(b_A)\sigma_{in}]^m \quad [\,1 - T_A(b_A)\sigma_{in}]^{A-m} \ . \tag{4.18}$$

The basic nucleon-nucleon thickness function t can be approximated by a delta function and the probability function P can be simplified to be just products:

$$P(n,m,\vec{b}_B,\vec{b}) = \binom{B}{n} [T_B(b_B)\sigma_{in}]^n \quad [\,1 - T_B(b_B)\sigma_{in}]^{B-n}$$

$$\times \binom{A}{m}[T_A(\vec{b}+\vec{b}_B)\sigma_{in}]^m \quad [\,1 - T_A(\vec{b}+\vec{b}_B)\sigma_{in}]^{A-m} \ . \tag{4.19}$$

For many problems, the dynamics is insensitive to the spatial

transverse coordinates $\vec{b}_B$ of the tube but is more sensitive to the number of nucleon-nucleon collisions in the tube. One can then integrate the transverse coordinates $\vec{b}_B$ to obtain the probability for collisions of n nucleons in B with m nucleons in A at an impact parameter b :

$$P(n,m,b) = \int \frac{d\vec{b}_B}{\sigma_{in}} \binom{B}{n} [T_B(b_B)\sigma_{in}]^n [1 - T_B(b_B)\sigma_{in}]^{B-n}$$

$$\times \binom{A}{m} [T_A(\vec{b}+\vec{b}_B)\sigma_{in}]^m [1 - T_A(\vec{b}+\vec{b}_B)\sigma_{in}]^{A-m} . \quad (4.20)$$

The results of Eqs.(4.19) and (4.20) are useful expressions for nucleus-nucleus collisions.

V. MODELS OF NUCLEUS-NUCLEUS COLLISIONS

The study of the dynamics of a nucleus-nucleus collision has not yet reached a stage where such a process can be described from the first principle, starting with the theory of QCD. The phenomenon of hadronization and confinement are intimately related and a non-perturbative QCD description is necessary. Even with simple model interactions, a relativistic theory of a many-body system interacting and producing particles has not been worked out so that a quantitative description is available at present. The investigation of such a problem constitutes one of the most outstanding problems confronting the theory of nucleus-nucleus collision today.

In the absence of a well-developed theoretical description of the nucleus-nucleus collision, there are many different models which attempt to describe the interaction processes. Many of these models treat a nucleon as an excitable entity and quarks enter only as a part of a collective cluster. These models have achieved various degrees of success. There are also models which treat nucleus-nucleus collisions completely at the quark level[28]. For the low p_t phenomena, their success has been limited, as the process of hadronization, confinement and recombination cannot be well described. We shall discuss here those models which consider hadrons as a collective unit in nucleus-nucleus collisions. All these models assume a multiple-collision process such as the Glauber-type model, for the geometrical part of the collision process. The problem is reduced to a detailed description of the space-time dynamics of what occurs when n nucleons from the beam nucleus B collide with m nucleons from the target nucleus A. The models differ in their assumptions as to how the particles share their energies and where the sources of particle production are. All of these models assume that, in accordance with experimental observations, production of the non-leading particles occurs after the two nuclei have passed through each other. This peculiar behavior can be easily understood. After an inelastic collision,

the colliding nucleons need to be separated by a distance of the order of a Fermi in the C.M. system before particles can be produced. However, when this occurs, the baryons have already moved forward into a different spatial region away from the production zone. Consequently, the produced particles do not collide with the baryons of the incident nuclei.

5.1 The Lund Model for Nucleus-Nucleus Collisions

In the Lund model, it is assumed that for low-p_t phenomena, the hadrons are not transversely excited but are only logitudinally stretched. The hadrons undergoing interaction are otherwise independent of each other. The collision of n beam nucleons and m target nucleons will result in $m+n$ excited hadrons. These hadrons subsequently decay after collisions have been completed and are the sources of particle production. The decay of these stretched hadrons is analyzed in the same way as in the decay of a stretched q-$\bar{q}$ pair which has been previously worked out in the older version of the Lund model.

To be more specific, the major assumptions of the Lund model consist of the following :

1) The hadrons which participate in the collision are independent and are individually excited. It is conveninet to represent the momentum of a hadron by the light-cone momentum coordinates (P_+,P_-) where the forward light-cone momentum P_+ is the sum of its energy and its logitudinal momentum P_z while the backward light-cone momentum P_- is the difference $E - P_z$. In the collision of one hadron with ν nucleons, the initial light-cone momenta of these $\nu+1$ hadrons are

$$(P_{1+},\ m^2/P_{1+}) \quad \text{and} \quad (m^2/P_{i-},P_{i-}) \text{ for } i = 2,\ldots,\nu+1 \ .$$

Collisions between the baryons will lead to the sharing of their momenta, but there is otherwise no quantum number flow from one baryon to another. After collision, the ith target baryons in the set $\{2,\ldots,\nu+1\}$ gain a momentum Q_{i+} in the forward light-cone

direction but lose a momentum Q_{i-} in the backward light-cone direction. The resultant momenta are

$$(m^2/P_{i-} + Q_{i+}, P_{i-} - Q_{i-}) \quad \text{for} \quad i = 2,\ldots,\nu+1 \tag{5.1}$$

and the momentum of the incident baryon is

$$(P_{1+} - \sum_{i=2}^{\nu+1} Q_{i+},\ m^2/P_{1-} + \sum_{i=2}^{\nu+1} Q_{i-}) \ . \tag{5.2}$$

2) It is assumed that the momentum transfer obeys a probability distribution given by

$$Probability = \frac{dQ_{i+}\ dQ_{i-}}{(m_1^2/P_{1+} + Q_{i+})\ (m_i^2/P_{i-} + Q_{i-})} \tag{5.3}$$

where the mass term comes from the lower limits of momentum transfer while the dQ/Q type of probability distribution comes from the Feynman parametrization of the momentum distribution of the wee-partons.

3) For nucleus-nucleus collisions, the above procedure is similarly generalized. That is, in each binary collision of the projectile baryon with momentum (P_{b+},P_{b-}) and a target baryon with momentum (P_{a+},P_{a-}), there is an exchange of momentum Q_+ and Q_- to result in the momentum $(P_{b+} - Q_+,P_{b-} + Q_-)$ for the projectile baryon and the momentum $(P_{a+} + Q_+,P_{a-} - Q_-)$ for the target nucleon. The only restriction is that Q_+ and Q_- must be greater than zero so that the dominant component of the momentum $P_{b+} - Q_+$ of the projectile baryon and $P_{a-} - Q_-$ of the target baryon will always decrease in their magnitudes after collision. The probability distribution of the exchange momentum is given by Eq. (5.3).

4) After the baryons complete their collisions, each excited baryon is then studied to obtain the spectrum of the produced particles. It is assumed that the decay of a final baryon with a momentum (P_{i+},P_{i-}) is similar to the decay of a $q\text{-}\bar{q}$ system with a massless quark traveling in the forward light-cone direction with a light-cone momentum P_{i+} and an anti-quark traveling to the backward light-cone direction with momentum P_{i-}. A previous Lund model for nucleon-nucleon collisions can be used for that purpose.

The Lund model for nucleus-nucleus collisions has been proposed only recently; it will be tested with the new data to examine the validity of the model.

5.2 THE DUAL-PARTON MODEL

The dynamics in the interaction of hadrons in a nucleus is described as proceeding in a different way in the dual-parton model developed by Capella, Tran Thanh Van, and their collaborators[29]. For the collision of one hadron against another hadron, the dual-parton model contains the following assumptions:
1). Each hadron is considered to consist of two elementary constituents. In the case of a meson, the constituents are a quark and an anti-quark; in the case of a baryon, the constituents are a quark and a di-quark. One infers the forms of the momentum distribution of these constituents inside the hadrons from other empirical considerations such as the dual resonance model. Specifically, the momentum distribution of the valence quark f_v, and the di-quark f_{qq} are assumed to be

$$f_v(x) = (x^2 + \mu^2 / p^2)^{-1/4}$$

and

$$f_{qq}(x) = x^{1.5} .$$

It is worth noting that the constituent partons here are not the same as the partons in the deep-inelastic scattering processes. They are "dual partons" which are assumed to contain features of the non-perturbative QCD.
2). In a collision of these two hadrons, these constituents fragment into the detected particles according to certain assumed empirical fragmentation functions. For example, the fragmentation functions for the valence quarks , and the di-quark to fragment into π^+ are respectively

$$xD(v \to \pi^+) = 0.5\ (1+x)F(x)$$

and

$$xD(qq \to \pi^+) = 0.675\ (1-x)^2 ,$$

where

$$F(x) = [\ 1.3(1-x)^2+0.05\ ] / (1-0.5x) \quad .$$

The resultant momentum distribution of the detected particle is just a folding of the momentum distribution of the constituents and the momentum distribution of the fragments coming from the constituents.

Upon choosing the structure functions and the fragmentation functions to fit experimental hadron-hadron data, the model is then used to study hadron-nucleus, baryon-nucleus, and nucleus-nucleus collisions with additional assumptions about the sea quark. For example, in the collision of a baryon with a nucleus, the collision is assumed to proceed in the following way, as shown in Figure 9 below:

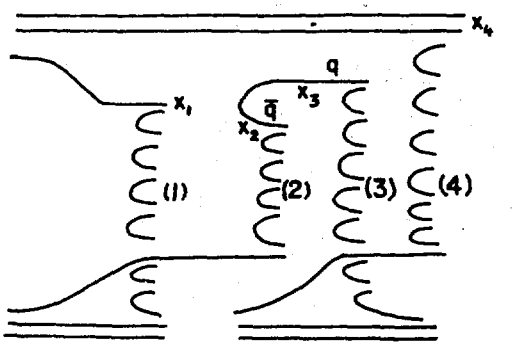

Fig. 9 Quark dynamics in the dual parton model.

It is assumed that the di-quark system of the incident baryon proceeds forward and develops a chain with a valence quark of the last struck nucleon (Chain 4 in Figure 9), while its valence quark develops a chain with the di-quark system of the first struck nucleon. The valence quarks of the target nucleons develop chains with the sea-quarks of the projectile nucleons. (Chains 2

and 3 in Figure 9). There are therefore two types of chains: those not involving sea quarks and those involving sea-quarks. In a collision of a baryon with n target nucleons, there are two chains not involving sea-quarks and $2n$-2 chains involving sea quarks. Each chain leads to independent productions of particles.

The momentum distribution of the sea-quark is assumed to be given by a distribution of a form which goes as 1/x as $x \to 0$:

$$f_s(x) = (x^2 + \mu^2 / p^2)^{-1/2} .$$

The sea quarks fragment into hadrons according to a prescribed fragmentation function. For example, the fragmentation function for a sea quark to go into a π^+ is assumed to be of the form

$$xD(s \to \pi^+) = F(x) ,$$

where $F(x)$ has been given previously in the expression for $xD(\nu \to \pi^+)$.

With the introduction of the sea quark, the momentum distribution of the produced particles can be obtained by a convolution. While the dual-parton model has been applied to some (light nucleus)-(light nucleus) collisions,[29] it will be tested with the new heavy-ion data from CERN.

5.3 THE MULTI-CHAIN MODEL

A different multiple-collision model, the multi-chain model was proposed by Kinoshita, Minaka, and Sumiyoshi[30]. In this model for a baryon-nucleus collision, incident baryons make collisions with many nucleons in the target nucleus. Each collision leads to the formation of a chain which later evolves into produced particles. The leading cluster degrades its momentum as the collision process proceeds. How the leading cluster loses energy is taken to be an unknown and parametrized function $P(x)$ to be determined by experiment. A convenient parametrization of the probability function $P(x)$ is taken to be

$$P(x) = \alpha x^{\alpha+1}$$

where x is the light-cone variable of the leading cluster. Other methods of partitioning the light-cone momentum have also been attempted. The momentum degradation of the leading cluster is assumed to be sequential so that the momentum distribution after n collisions is the folding of the momentum distribution after $n-1$ collisions and the probability function $P(x)$. After each collision, each chain also acquires a momentum fraction, and it decays into hadrons, depending on a fragmentation function G which is a function of the light-cone momentum of the chain. For example, for charged secondary particles, the fragmentation function was assumed to have the form:

$$G(z,x_-) = (1- z)^{\beta} (1-x_-)^{\alpha}$$

where z is the light-cone variable of the detected hadron relative to the chain and x_- is the light-cone variable of the detected hadron relative to the target nucleon.

5.4 Other Variations of the Multiple-Collision Model

Besides these models, there are many variations of the multiple-collision model which differ in the way the energy and the momentum of the particles are partitioned and the sources of particle production. In the approach taken by the present author[31], nucleons of one nucleus form leading clusters as they pass through and make successive collisions with nucleons in the other nucleus. The baryon clusters degrade their energy and momentum. It is assumed that an approximate description, subject to modifications, is that the leading clusters degrade energy and produce particles approximately as if they were in free space. Each collision is a source of produced particles. The energy loss in each collision leads to particle production as in free space, except that these secondary particles emerge only after the nucleus-nucleus collision has been completed. Consequently, the produced non-leading particles do not make collision with the projectile or the target nucleons. Results obtained with such a

model give a reasonable description of stopping power when a proton passes through a nucleus[31]. However, further tests and modifications of the simple model may be necessary to confront the new heavy-ion data that are emerging.

A similar approach has also been taken by Ludlam[32] and his collaborators, which results in the HIJET computer program. It is assumed in a similar way that the leading clusters in nucleus-nucleus collisions make successive collisions with nucleons of the other nucleus. In each collision, the energy loss and the spectrum of produced particles are calculated with the ISAJET program which has been written to reproduce the nucleon-nucleon collision data. While the leading clusters can continue on to make more collisions as they pass through the other nucleus, the produced particles emerge only after the nuclei are far apart and do not participate in secondary collisions. The HIJET program has been used as an event generator to aid the design of expermental detectors and has also been used to compare with preliminary experimental data.

VI. RELATIVISTIC HEAVY-ION COLLISIONS AND QUARK-GLUON PLASMA

From the experimental data in nucleon-nucleon collisions, we know that an inelastic nucleon-nucleon collision is accompanied by a large loss of the baryon energy which is released in the form of produced particles in the central rapidity region. In nucleus-nucleus collisions, the number of nucleon-nucleon collisions can be very large. For example, in the head-on collision of a uranium nucleus on another uranium nucleus, the number of inelastic baryon collisions is[27] about 800. The multiple collision models we discussed in the last section indicate that the effects of the many collisions are rougly additive. Lorentz contraction also makes the collisions to occur in a very small spatial region and in a small temporal extension. In consequence, when the incident energy is appropriate (at about a few GeV per nucleon in the C.M. system), the baryons in a nucleus may make so many collisions that the leading baryon clusters may be effectively stopped in the C.M. system. The stopping of the baryons gives rise to baryon matter of very high density and may lead to a transition from the confined baryon matter to the unconfined quark-gluon plasma with a large net baryon number density[33,34]. In the other extreme, at very high energies, the slowed-down baryons after the collision still have enough momentum to proceed forward. The energy lost by the baryons is released in the form of produced particles in the central rapidity region. As first suggested by Bjorken[35], the energy density there may be high enough to form a quark-gluon plasma with a small baryon content.

We shall first discuss the latter case when the incident energy is so high that the baryons are not effectively stopped in the center-of-mass system. We can infer the energy density from the rapidity density dN/dy of the produced particles[35]. For simplicity, we consider the head-on collision of two equal nuclei in the center-of-mass frame. There is a substantial Lorentz contraction in the logitudinal direction so that one can neglect

the longitudinal thickness of the nuclei in that frame. At a proper time t_0 of about 1 fm/c after the two nuclei collide with each other, the baryons will be separated by a distance of about 2 fm and the hadrons will be produced in the form of free particles. The longitudinal coordinate of a produced particle is related to its rapidity by

$$z = t_0 \tanh y \ . \qquad (6.1)$$

The energy ΔE contained in the region of thickness Δz between the two nuclei is

$$\Delta E = m_T \cosh y \ \frac{dN}{dy} \ \frac{dy}{dz} \ \Delta z \ , \qquad (6.2)$$

where m_T is the transverse mass ($\simeq$0.4 GeV) and $(m_T \cosh y)$ is the energy of the produced particle. Using Eq. (6.1), the energy density averaged over the overlapping area A of the colliding nuclei is

$$\epsilon = \frac{\Delta E}{A \ \Delta z} = \frac{dN}{dy} \ \frac{m_T}{t_0 A \ [1 - (z/t_0)^2 \ ]^{3/2}} \ . \qquad (6.3)$$

The proper energy density is defined in the frame in which the medium is at rest. The proper energy density of the matter at $y = 0$ (corresponding to the point $z = 0$) is therefore given by[35]

$$\epsilon = \frac{dN}{dy} \ \frac{m_T}{t_0 A} \ . \qquad (6.4)$$

In nucleus-nucleus collisions, experimental results and a simple multiple-collision model calculation[27] suggest that the effect of multiple collisions on the rapidity density dN/dy is accumulative and goes approximately as $A^{4/3}$. For the head-on collision of ^{238}U on ^{238}U at a center-of-mass energy of 30 GeV per nucleon, the energy density in the central rapidity region has been estimated[27] to be of the order of 5 GeV/fm^3.

We can compare this energy density with the energy density of matter in the quark-gluon plasma phase as predicted by the

lattice-gauge theory[36]. In the lattice-gauge theory calculations, there are the gauge fields and the fermion fields to be specified at the lattice sites. The calculations are much simplified in the pure gauge field theory with no dynamical quarks. It is found that the deconfinement transition in SU(2) and SU(3) pure gauge theories are respectively second[37] and first order[38]. For the SU(3) pure gauge theory, the deconfinement transition temperature is 200-230 MeV [39] and the latent heat is 1.89 GeV/fm^3.[40] In lattice gauge calculations with dynamical quarks, the effective action is complex and the usual Monte Carlo method, which depends on a positive-definite probability measure, becomes inapplicable. Various methods have been proposed but major numerical difficulties remain. Although there has been much progress,[41] reliable numerical results are not yet available. If the quark mass m_q is heavy, work done with the $1/m_q$ expansion (the hopping parameter expansion), show that a first-order deconfinement transition persists[42] and that the energy density of the quark-gluon plasma is of the same order as the Stefan-Boltzmann energy density of a free quark-gluon plasma[43]. The latter quantity is

$$\epsilon = \frac{\pi^2}{30} \left[2\times 8 + \frac{7}{8}\times 2\times 2\times 2\times 3 \right] T^4 \qquad (6.5)$$

where the first contribution inside the square bracket comes from the 8 gluons and the second contribution comes from the quarks and antiquarks with two favors, two spins and three color degrees of freedom. Thus, if the transition temperature is 200 MeV, the energy density of the pure quark-gluon plasma is of the order of 2.5 GeV/fm^3. However, the masses of the dynamical quarks in a full QCD calculation are not large. Results from the hopping parameter expansion can be only a qualitative estimate for the full QCD dynamics. Nevertheless, the estimated energy density achievable in high-energy heavy-ion collisions is about the same as the estimated energy density of the quark-gluon plasma at the transition temperature. High-energy heavy-ion collision may

provide a tool to meet one of the requirements for quark-gluon plasma production.

We turn now to discuss the possibility of using high-energy heavy-ion collisions to produce a quark-gluon plasma with a high baryon number content[33,34]. We can examine the dynamics of the baryons in the center-of-mass system. The baryons of one nucleus lose a large fraction of their logitudinal kinetic energy in their collisions with the baryons of the other nucleus. The kinetic energy of the baryons may be degraded so much that they are essentially stopped in the center-of-mass system. It is possible to make an estimate of the degree of stopping in such a case with the multiple-collision model. The slowing-down of a nucleon in its passage through another nucleus can be considered as arising from a series of successive collisions, each collision resulting in a loss of the momentum fraction x as if it would occur in free space[31]. With such a model, we show in Fig. 10, a typical

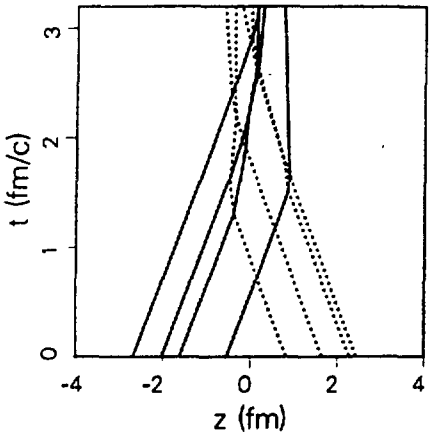

Fig. 10 Space-time dynamics of colliding rows of baryons at a laboratory energy of 15 GeV per nucleon.

space-time dynamics of the baryons in the collision of a tube of 4 nucleons (solid lines) with another tube of four nucleons (dashed lines) in the center-of-mass system for the incident laboratory energy of 15 GeV per nucleon[34]. After the collisions have

finished, the baryons have small velocities and the baryon density is large. The spatial density is about one order of magnitude larger than the nuclear matter density at equilibrium. The inclusion of mutual repulsion for baryon matter at high density would reduce the maximum density achieved. Nevertheless, there is a compression of the nuclear matter due to the slowing-down of the baryons. Such a compression may produce baryon matter of high density exceeding the baryon density for a phase transition from the confined baryon matter to the unconfined quark-gluon plasma with a high baryon number content.

With the experimental facilities capable of accelerating heavy ions to very high energies coming online, many proposals have been put forth to search for the state of a quark-gluon plasma (see reference 1 for the latest reviews of this subject). It is generally recognized that there is no unique single signal which allows an unequivocal identification of the quark-gluon plasma phase. What can be achieved may be an accumulative set of evidences which taken together may hopefully indicate the presence of the quark-gluon plasma phase.

One type of experiment suggests the examination of the equation of state of the quark-gluon plasma by studying the temperature and energy density relationship. As temperature can be measured by the average transverse momentum and the energy density measured by the rapidity density dN/dy at the rapidity plateau, a correlation of p_T and dN/dy may reveal the peculiarity of a phase transition. Specifically, there should be a large range of the energy density over which there is a very small change of the equilibrium temperature. If there is no change of the temperature, the transition is a first order transition. If there is a small change in equilibrium temperature, then the transition is a second order transition.

Another suggested signal is the use of strangeness production to infer whether the quark-gluon plasma phase has been reached. With the formation of a quark-gluon plasma, a chemical and thermal

equilibrium will allow the presence of substantial content of the strangeness. This is because the critical temperature and the mass of the strange quark are comparable. In contrast, hadronic matter consists mainly of pion gas and has little strangeness content. Another useful property is that after the quark-gluon plasma phase has been reached and hadronization has taken place, the strangeness content cannot be eliminated except by annihilation with another anti-stange quark which occurs only rarely. To measure the strangeness content, it is best to detect anti-hyperons and the more favorable case is in a baryon-rich quark-gluon plasma. The use of a K/π ratio is not a good signature as this ratio is fixed by the entropy content and not so much by the chemical and thermal equilibrium in the quark-gluon plasma phase.

Leptons and photons interact only weakly with hadrons. It has been suggested that one uses di-lepton pairs and direct photons as a probe of the quark and antiquark density and the temperature in the quark-gluon plasma phase. When quarks or quarks and antiquark interact to produce these particles, their reaction rates depend on the quark density and the quark temperature. Lepton pairs from the quark-gluon plasma phase should be dominant in the lower mass region between 300 and 500 MeV and could be a very sensitive measure of the temperature reached in the plasma phase.

It has also been suggested that one may use pion interferometry to extract the temperature parameter, effective source lifetime and transverse size. Other signals involve the use of meson and baryon momentum distributions and fluctuations to detect the hydrodynamical expansion.

VII DISCUSSIONS

Previous experimental investigations of high energy heavy-ion collisions used only cosmic ray particles as the source of projectiles. Much qualitative information has been obtained from these studies.[44] It is only recently that we are able to accelerate heavy-ions to many tens of GeV per nucleon at Brookhaven and at CERN. Future plans call for the possible construction of a relativistic heavy-ion collider capable of accelerating nuclei to an energy of 100 GeV per nucleon in the center-of mass system. A new field of physics has been opened up for quantitative investigation.

There are roughly two different but related aspects of high energy heavy-ion physics. On the one hand, it provides a special arena to examine the relativistic hadron dynamics and the process of particle production. On the other hand, it can be used as a tool for the possible production of matter with high energy density or high baryon number content in which the constituent quarks are not confined.

Nucleus-nucleus collisions differ from nucleon-nucleon collisions in many respects. There is now the new degree of freedom in the presence of other participating nucleons following a single nucleon-nucleon collision. One elementary nucleon-nucleon collision may not have finished before another elementary collision begins. The presence of many nucleons participating in a chain of collisions gives rise to shadowing effects and interference of the elementary particle production processes. How one can describe the mechanics of such a relativistic many-body problem in terms of simple, basic physical principles constitutes a major challenge of high-energy heavy-ion physics. The phenomenological models available so far serve to abstract the important aspects of the physics involved. They serve useful purposes but many problems remain. For example, the break-up probability in the Lund model is given by a function $f(z)$ which is obtained by requiring it to reproduce the empirical multiplicity

distribution and the symmetry of breaking the string from the left and from the right. It may be useful to work out the break-up probability for a string with a Schwinger-type model having rapidly moving boundaries. Likewise, the exchange of momenta between two colliding baryons in the Lund model for heavy-ions follows an assumed probability distribution. It is desirable to work out whether the dynamics of model strings or vortex lines indeed follows space-time motion of the prescribed type.

Aside from the question of the dynamics of the collision processes, high energy heavy-ion collisions may provide the tool to produce a quark-gluon plasma because of the high energy density that can be achieved. The high energy density is expected because of the accumulative effect of many collisions occurring in a small spatial region in a small temporal extent. Future experimental investigations include the search and the identification of the quark-gluon plasma. If it would be detected, more experimental investigations would be needed to examine its properties. The study of the quark-gluon plasma constitutes another major challenge of high-energy heavy-ion physics.

As of now, experimental information from the few experiments at Brookhaven with ^{16}O ions at 15 GeV per nucleon and at CERN with ^{16}O ions at 60 GeV and 200 GeV per nucleon indicate that a large number of particles are produced carrying away a large fraction of the incident energy. For example, in the collision of ^{16}O on Au at a laboratory energy of 200 GeV per nucleon, a maximum total multiplicity of 300 has been observed. The rapidity density is high and suggests that an energy density of the order of 2-3 GeV/fm^3 has been achieved.[45] For a collision of two nuclei with mass numbers A and B, the energy density goes as $AB/(A^{1/3}+B^{1/3})$.[24] There will be a substantial increase in the energy density when the projectile mass is increased. Future use of heavier projectiles will facilitate the production of the quark-gluon plasma, if there is indeed a phase transition from a hadron matter to a quark-gluon plasma.

ACKNOWLEDGEMENT

The author would like to thank Drs. Renchuan Wang and Zhong-dao Lu for helpful discussions. This research was supported by the Division of Nuclear Physics, U.S. Department of Energy under Contract No.DE-AC05-84OR21400 with Martin Marietta Energy Systems, Inc.

REFERENCES

1. For a review of current research, see Proceedings of the International Conference on Ultra-Relativistic Nucleus-Nucleus Collisions, Asilomar, 1986, published in Nuclear Physics A461 (1987); *Quark Matter* '84, Proceedings, Helsinki Quark Matter Conference 1984, Edited by K. Kajantie, Springer-Verlag, Berlin, 1985.
2. *The First Three Minutes*, S. Weinberg, Basic Books,N.Y.,1977.
3. W. Thomé, *et. al.*, Nucl. Phys. B129, 365 (1977).
4. K. Alpgard *et. al.* ,Phys. Lett. 107B, 310 (1981).
5. A. E. Brenner *et. al.*,Phys. Rev. D26, 1497 (1982).
6. J. Schwinger, Phys. Rev. 82, 664 (1951);
   E. Brezin and C. Ityzkson, Phys. Rev. D2, 1191 (1970).
7. A. Casher, J. Kogut, and L. Susskind, Phys. Rev. D10, 732 (1974); A. Casher, H.Neuberger and S.Nussinov, Phys. Rev. D20, 179 (1979); H. Neuberger, Phys. Rev. D20, 2936 (1979); C.B. Chiu and S. Nussinov, Phys. Rev. D20, 945 (1979); I.K. Affleck *et. al.*, Nucl Phys. B197, 509 (1982).
8. A comprenhensive review of the Lund Model can be found in B. Andersson, G. Gustafson, G. Ingelman, and T. Sjöstrand, Phys. Rep. 97, 31 (1983); other references on the Lund model: T. Sjöstrand, Comp. Phys. Comm. 39, 347 (1986); B. Andersson *et. al.* Z. Phys. C1, 105 (1979); B. Andersson *et. al.* Z. Phys. C20, 317 (1983);
9. E. Ley Koo, Wang Renchaun, Ren Shangfeng, Sun Zongyang, Hua Xinmin, Jour. China Univ. of Sci. Tech. 13, 167 (1983)

10. T. Sjöstrand, Comp. Phys. Comm. 39, 347 (1986);
11. Renchuan Wang, C.Y. Wong, P. Siemens, and C.M. Ko,(to be published)
12. *Handbook of Mathematical Functions*, ed. M. Abramowitz and I. A. Stegun, Dover Publications, N.Y., 1965.
13. J. Schwinger, Phys. Rev. 128, 2425 (1962);
J. Schwinger, Lecture Presented at Seminar on Theoretical Physics, Trieste, 1962, published by IAEA, Vienna, 1963, p.89.
14. X. Artru and G. Mennessier, Nucl. Phys. B70, 93 (1974);
B. Andersson, Phys. Rep. 97, 31 (1983);
X. Artru, Phys. Rep. 97, 147 (1983).
15. J. D. Bjorken, Lectures presented in the 1973 Proceedings of the Summer Institute on Particle Physics, edited by Zipt, SLAC-167 (1973);
A. Casher, J. Kogut, and L. Susskind, Phys. Rev. D10, 732 (1974);
16. R.D. Field and R. P. Feynman, Nucl. Phys. B136, 1 (1978).
17. C. Petterson *et. al.*, Phys. Rev. D27, 105 (1983).
18. Ch. Berger *et. al.* (PLUTO Collaboration), Phys. Lett. 95B, 313 (1980); W. Bartel *et. al.* (JADE Collaboration), DESY 83-042
19. B. Andersson, G. Gustafson and B. Nilsson-Almqvist, Nucl. Phys. B281, 289 (1987).
20. B. Nilsson-Almqvist and E. Stenlund, Comp. Phys. Comm. 43, 387 (1987).
21. C.Y. Wong (unpublished).
22. R.P. Feynman, Phys. Rev. Lett. 23, 1415 (1969).
23. F. E. Taylor *et. al.*, Phys. Rev. 14, 1217 (1976).
24. C. Y. Wong, Phys. Rev. 30, 972 (1984).
25. M. Basile *et. al.*, Nuovo Cimento 65A, 400 (1981);
M. Basile *et. al.*, Nuovo Cimento 67A, 244 (1981).
26. R. J. Glauber, in Lectures in Theoretical Physics, edited by W. E. Brittin and L. G. Dunham (Interscience, N.Y., 1959), Vol. 1, p. 315.
27. C. Y. Wong, Phys. Rev. D30, 961 (1984).
28. R. C. Hwa, Phys. Rev. Lett. 52, 492 (1984); R. C. Hwa and M. S.

Zahir, Phys. Rev. D31, 499 (1985).
29. A. Capella and A. Krzywicki, Phys. Rev. D18, 3357 (1978); A. Capella and J. Tran Thanh Van, Z. Phys. C10, 249 (1981); A. Capella, C. Pajares and A.V. Ramallo, Nucl. Phys. B241, 75 (1984); A. Capella,A. Staar and J.Tran Thanh Van, Phys. Rev. D32, 2933 (1985); A. Capella *et. al.*, Z. Phys. C33, 541 (1987).
30. K. Kinoshita, A. Minaka, and H. Sumiyoshi, Prog. Theo. Phys. 63, 1268 (1980).
31. C. Y. Wong, Phys. Rev. Lett. 52, 1393 (1984); C.Y. Wong, Phys. Rev. D30, 972 (1984); C.Y. Wong D32, 94 (1985).
32. T. W. Ludlam, (unpublished)
33. A. S. Goldhaber, Nature 275 114 (1978); R. Anishetty, P. Koehler, and L. McLerran, Phys. Rev. D22, 2793 (1980); J. Kapusta, Phys. Rev. C27, 2037 (1983); W. Busza and A. S. Goldhaber, Phys. Lett. 139A, 235 (1984); M. Gyulassy, Phys. Rev. D30, 961 (1984);
34. C. Y. Wong, Phys. Rev. C33, 1340 (1986).
35. J. D. Bjorken, Phys. Rev. D27, 140 (1983).
36. H. Satz, Nucl. Phys. A418, 447c (1984); T. DeGrand, in *Quark Matter* '84, Proceedings, Helsinki Quark Matter Conference 1984, Edited by K. Kajantie, Springer-Verlag, Berlin, 1985, p. 17. B. Svetitsky, Nucl. Phys. A461, 71c (1987).
37. L. Susskind, Phys. Rev. D20, 2610 (1979); A. Polyakov, Phys. Lett. 72B, 477 (1978); L. McMerran and B. Svetitsky, Phys. Rev. D24, 450 (1981) J. Polyonyi *et. al.*, Phys. Lett. 98B, 195 (1981).
38. L. Yaffe and B. Svetitsky, Phys. Rev. D26, 963 (1982); B. Svetitsky and L. Yaffe, Nucl. Phys. B210, 423 (1982).
39. S. A. Gottlieb *et. al.*, Phys. Rev. Lett. 55, 1958 (1985).
40. F. Fucito and B. Svetitsky, Phys. Lett. 131B, 165 (1983).
41. J. B. Kogut, Nucl. Phys. A461, 327c (1987).
42. J. Polonyi and H. W. Wyld, Phys. Rev. Lett. 51, 2257 (1983); J. Polonyi *et. al.*,Phys. Rev. Lett. 53, 644 (1984);

S. Duane, Nucl. Phys. B257[FS14], 652 (1985);
S. Duane and J. Kogut, Phys. Rev. Lett. 55, 2774 (1985);
T. Banks and A. Ukawa, Nucl. Phys. B225, 145 (1983);
T. DeGrand and C. DeTar, Nucl. Phys. B225, 590 (1983).

43. J. Engels, Nucl. Phys. A461, 317c (1987).

44. JACEE Collaboration, Phys. Rev. Lett. 50, 2062 (1983);
JACEE Collaboratory, in *Quark Matter* '84, Proceedings, Helsinki Quark Matter Conference 1984, Edited by K. Kajantie, Springer-Verlag, Berlin, 1985, p. 187;
JACEE Collaboration, Nucl. Phys. A461, 263c (1987).

45. R. Brockmann, Lecture given at this Spring School, April 1987;
R. Brockmann, Proceeding of the 11th PANIC Conference at Kyoto, April 1987, to be published.
D. A. Lissauer, Proceeding of the 11th PANIC Conference at Kyoto, April 1987, to be published.
O. Hanson, Proceeding of the 11th PANIC Conference at Kyoto, April 1987, to be published.